

Cooling a spherical nematic shell

Gaetano Napoli

Dipartimento di Matematica e Fisica "E. De Giorgi", Università del Salento, Lecce, Italy

Luigi Vergori

Dipartimento di Ingegneria, Università degli Studi di Perugia, Perugia, Italy

Within the framework of Landau-de Gennes theory for nematic liquid crystals, we study the temperature-induced isotropic-nematic phase transition on a spherical shell. Below a critical temperature, a thin layer of nematic coating a microscopic spherical particle exhibits non-uniform textures due to the geometrical frustration. We find the exact value of critical threshold for the temperature and determine exactly the nematic textures at the transition by means of a weakly nonlinear analysis. The critical temperature is affected by the extrinsic curvature of the sphere, and the nematic alignment is consistent with the Poincaré-Hopf index theorem and experimental observations. The stability analysis of the bifurcate textures at the isotropic-nematic transition highlight that only the tetrahedral configuration is stable.

PACS numbers:

Many physical systems exhibit intriguing patterns and textures whose understanding and control is a central goal across many areas of science and engineering. One category of pattern-forming is provided by nematic shells, which consist in nematic liquid crystals (LCs) confined on a self-closing spherical shell. The constraint imposed by such confinement combined with degenerate anchoring of the nematic at the interfaces inevitably results in the presence of topological defects, i.e. regions where the orientational order of the liquid crystal is disrupted. The seminal idea of Nelson [1] of mimicking atomic properties at microscopic scale by functionalizing defects of nematic shells has led to a vivid research activity in the last two decades, both theoretical [2–12] and experimental [13–16]. Moreover, recent advances in microfluidics techniques [14, 15, 17, 18] have made it possible to prepare long-term stable liquid crystalline (LC) shells which, in turn, has enabled the application of LC shells in the design of innovative devices in the fields of photonics [19, 20], biosensing [21] and micromechanics [22].

Nematic LCs are fluids with orientational order and no long-range positional order. The Landau-de Gennes theory for nematic LCs (the most widely used model to describe the thermomechanical response of LCs) is based on the orientational probability distribution of molecules and uses a symmetric traceless second order tensor \mathbf{Q} to characterize this distribution. For nematic LCs occupying a thin shell it has been shown that, upon appropriate chemical treatments of the shell interfaces, a fully tangential, a fully normal or a hybrid alignment can be achieved in the bulk [23]. Within the hypothesis of fully tangential alignment and constant thickness, a surface free energy for nematic shells has been derived from the Landau-de Gennes model by means of a perturbation technique [8]. In what follows we shall refer to this surface free energy as the surface Landau-de Gennes potential. Within this setting \mathbf{Q} degenerates consistently with the tangential distributions of the average directions of the molecules. These degenerate states are described by the tangential

order tensor \mathbf{Q}_s which, with respect to a local basis on the shell surface, is represented by a 2×2 traceless symmetric matrix [3].

We shall henceforth consider a spherical surface, and let $\phi \in [0, 2\pi)$ and $\theta \in [0, \pi]$ be the longitude and the colatitude, respectively. With respect to the local basis $\{\mathbf{e}_\phi, \mathbf{e}_\theta\}$, the components of the tangential order-tensor \mathbf{Q}_s form the matrix

$$[\mathbf{Q}_s] = \begin{pmatrix} q_0 & q_m \\ q_m & -q_0 \end{pmatrix},$$

where $q_0(\phi, \theta)$ and $q_m(\phi, \theta)$ are two scalar fields the admissible values of which lie within the disc centered at the origin of the q_0q_m -plane with radius $1/2$ [7]. Any in-plane directional ordering is lost wherever both q_0 and q_m vanish. If this is the case, the nematic is in the two-dimensional isotropic phase. Otherwise, the unit eigenvector of \mathbf{Q}_s corresponding to the greatest eigenvalue yields the average direction of the molecules. Following [7], the angle contained between such an average direction and the principal direction \mathbf{e}_ϕ on the sphere is equal to $[\arctan(q_m/q_0)]/2$ if $q_0 \geq 0$, or $[\pi + \arctan(q_m/q_0)]/2$ if $q_0 < 0$.

Earlier studies have shown how the extrinsic curvature of the shell affects the ordering of the molecules [8, 9]. In particular, it has been proven that uniform in-plane isotropic states, *i.e.* states for which \mathbf{Q}_s vanishes everywhere, may occur only on surfaces with zero local asphericity or zero mean curvature [24]. Uniform flat isotropic states may then occur on the sphere and minimal surfaces. In this Letter, we study the effects of lowering the temperature in a nematics confined to a spherical shell. Initially the temperature is high enough that there is no in-plane preferred direction. The nematic order occurs as soon as the temperature reaches a critical value which we shall determine exactly by employing the surface Landau-de Gennes potential.

This potential is in the form $W = \int_S w_a$, where S is a sphere of radius r and the surface energy density w is

the sum of the surface elastic (w_{el}) and the Landau-de Gennes (w_{LdG}) energy densities [8].

Within the one-constant approximation, w_{el} takes the form

$$w_{el} = \frac{k}{2} (|\nabla_s q_0 + 2q_m \boldsymbol{\omega}|^2 + |\nabla_s q_m - 2q_0 \boldsymbol{\omega}|^2) + \frac{k}{r^2} (q_0^2 + q_m^2), \quad (1)$$

where $k > 0$ is the reduced elastic stiffness, and $\boldsymbol{\omega}$ is the vector parametrizing the spin connection on the sphere [25]. In spherical coordinates, the vector parametrizing the spin connection and the surface gradient operator read $\boldsymbol{\omega} = r^{-1} \cot \theta \mathbf{e}_\phi$ and $\nabla_s = [(r \sin \theta)^{-1} \partial_\phi] \mathbf{e}_\phi + [r^{-1} \partial_\theta] \mathbf{e}_\theta$, respectively.

The Landau-de Gennes energy density w_{LdG} is quartic in q_0 and q_m and given by

$$w_{LdG} = \frac{a}{2} (q_0^2 + q_m^2) + \frac{c}{4} (q_0^2 + q_m^2)^2, \quad (2)$$

where $a = a_0(T - T_{NI})/T_{NI}$, a_0 and c are positive constants and T denotes the absolute temperature. The quantity T_{NI} represents the nematic-isotropic transition temperature for planar nematics [8].

We now introduce the complex variable $q = q_0 + iq_m$ so that the total energy density w becomes

$$w = \frac{k}{2} |\nabla_s q - 2iq\boldsymbol{\omega}|^2 + \underbrace{\frac{a_{\text{eff}}}{2} |q|^2 + \frac{c}{4} |q|^4}_{\equiv w_{LdG}^{\text{(eff)}}}, \quad (3)$$

where $a_{\text{eff}} = a + 2k/r^2$ depends not only on the constitutive properties of the nematics, but also on the extrinsic curvature of the sphere. Thus, the energy density $w_{LdG}^{\text{(eff)}}$ can be regarded as the effective thermal potential on the sphere.

Following the variational scheme introduced in [26], the (dimensionless) Euler-Lagrange equation associated with the surface Landau-de Gennes potential is found to be

$$\mathcal{L}q - \bar{a}q - \bar{c}|q|^2q = 0, \quad (4)$$

where $\mathcal{L} = r^2(\Delta_s - 4i\boldsymbol{\omega} \cdot \nabla_s - 4|\boldsymbol{\omega}|^2)$, $\Delta_s = (r \sin \theta)^{-2} \partial_\phi^2 + r^{-2}(\sin \theta)^{-1} \partial_\theta(\sin \theta \partial_\theta)$ is the Laplace-Beltrami operator on the sphere, $\bar{a} = a_{\text{eff}}/k$ and $\bar{c} = c/k$. It is immediate to check that (4) admits the trivial solution $q = 0$ (which corresponds to the in-plane isotropic state) for any values of \bar{a} and \bar{c} . However, as the temperature decreases, \bar{a} becomes smaller and smaller, and, as soon as it reaches a critical value, the trivial solution becomes unstable. The onset of nematic ordering occurs then as a bifurcation from the trivial solution.

To study this bifurcation problem, we expand q as a power series in the dimensionless parameter $\varepsilon = \sqrt{\bar{a}/\bar{a}_{\text{cr}}} - 1 \ll 1$ that provides a measure of the small departures of \bar{a} from its value \bar{a}_{cr} at the nematic-isotropic transition temperature T_{cr} on the sphere. For small temperature departures from T_{cr} , we then look for solutions of (4) in the form $q = \sum_{n=1}^{+\infty} \varepsilon^n q_n$.

To leading order, q_1 satisfies the linear equation

$$\mathcal{L}q_1 = \bar{a}q_1. \quad (5)$$

Since the differential operator $-\mathcal{L}$ is self-adjoint and positive, its spectrum is countable and its eigenvalues are real and positive. More precisely, the spectrum of $-\mathcal{L}$ is the set $\{\lambda_n = n^2 + n - 4 : n \in \mathbb{N}, n \geq 2\}$, whence $\lambda_2 = 2$ is the least eigenvalue of $-\mathcal{L}$. As a direct consequence, equation (5) admits a non-trivial solution if and only if $\bar{a} \leq \bar{a}_{\text{cr}} = -2$, which implies that the in-plane isotropic state $q = 0$ is stable if and only if $\bar{a} > \bar{a}_{\text{cr}} = -2$ or, equivalently in view of the definitions of a and a_{eff} ,

$$T > T_{\text{cr}} = T_{\text{NI}} \left(1 - \frac{4k}{a_0 r^2} \right). \quad (6)$$

The extrinsic curvature curvature has then the effect to make the nematic-isotropic transition temperature on the sphere be lower than that for planar nematics.

The smooth eigenfunctions of $-\mathcal{L}$ corresponding to the least eigenvalue $\lambda_2 = 2$ can be written in terms of complex trigonometric functions (normalized on using the Hermitian inner product $\langle u, v \rangle = \int_S uv^* \mathfrak{a}$, where the superscript $*$ denotes the complex conjugate) as

$$\begin{aligned} f_{-2} &= \frac{1}{2} \sqrt{\frac{5}{\pi}} \exp(-2i\phi) \sin^4 \frac{\theta}{2}, \\ f_{-1} &= \sqrt{\frac{5}{\pi}} \exp(-i\phi) \sin^3 \frac{\theta}{2} \cos \frac{\theta}{2}, \\ f_0 &= \sqrt{\frac{15}{2\pi}} \sin^2 \frac{\theta}{2} \cos^2 \frac{\theta}{2}, \\ f_1 &= \sqrt{\frac{5}{\pi}} \exp(i\phi) \cos^3 \frac{\theta}{2} \sin \frac{\theta}{2}, \\ f_2 &= \frac{1}{2} \sqrt{\frac{5}{\pi}} \exp(2i\phi) \cos^4 \frac{\theta}{2}. \end{aligned} \quad (7)$$

The bifurcate solutions are then linear combinations of these five modes

$$q_1 = \sum_{h=-2}^2 A_h f_h, \quad (8)$$

where $A_h = \varrho_h \exp(i\psi_h)$ are arbitrary complex constants. These are to be determined by taking into account the non-linear term in (4) that has thus far been neglected. Taking into account that $\bar{a}_{\text{cr}} = -2$ and the definition of ε , for small temperature departures from the critical value (6) we have $\bar{a} = -2(1 + \varepsilon^2)$. Thus, collecting terms of order $O(\varepsilon^3)$ in the equilibrium equation (4), with q expanded as a power series in ε , gives the equation $(\mathcal{L} + 2)q_3 = (2 - \bar{c}|q_1|^2)q_1 \equiv g$. On using the Lyapunov-Schmidt reduction [27] and in view of the self-adjointness of \mathcal{L} , this equation is solvable providing that g belongs to the orthogonal complement of the kernel of $\mathcal{L} + 2$. In other words, we have to require that $\langle g, f_h \rangle = 0$ for all $h = -2, \dots, 2$. These conditions yield a system of

five nonlinear algebraic equations in the five unknowns $A_h = \varrho_h \exp(i\psi_h)$.

On the other hand, the Poincaré-Hopf index theorem guarantees that on a spherical nematic shell there must be at least one melting point. Therefore, without loss of generality, we can limit our bifurcation analysis to linear combinations (8) that vanish at the north pole, i.e. for $\theta = 0$. This ansatz reduces by one the number of unknowns and equations in the system of nonlinear algebraic equations $\{\langle g, f_h \rangle = 0 : h = -2, \dots, 2\}$. Indeed, since f_2 does not vanish at the north pole we take $A_2 = 0$ in (8) and release the condition $\langle g, f_2 \rangle = 0$. The resulting reduced system of nonlinear algebraic equations admits infinitely many solutions, each of which determines uniquely a bifurcate texture.

Within the Landau-de Gennes theory, defects are melting points, i.e. isolated points where q vanishes. According to the number of the melting points and their distribution on the spherical shell, the bifurcate textures can be divided into seven broad classes of configurations.

- (\mathcal{C}_1) Monovalent: a single $m = +2$ melting point.
- (\mathcal{C}_2) Linear non-axisymmetric: two antipodal melting points with topological charges $+1/2$ and $+3/2$.
- (\mathcal{C}_3) Linear axisymmetric: two $m = +1$ antipodal melting points.
- (\mathcal{C}_4) Trigonal: three melting points located at the vertices of an isosceles triangle on a maximum circle on the sphere, two of them with $m = +1/2$ and the other with $m = +1$. The base angles of the isosceles triangle measure $\alpha_1 = \arctan \sqrt[4]{40} \approx 68.315^\circ$ and the vertex angle measures $\alpha_2 = \pi - 2\arctan \sqrt[4]{40} \approx 43.37^\circ$. The values of α_1 and α_2 are in perfect agreement with the experimental results reported in [14].
- (\mathcal{C}_5) Tetrahedral: four $m = +1/2$ melting points located at the vertices of a regular tetrahedron.
- (\mathcal{C}_6) Squared: four $m = +1/2$ melting points situated at the vertices of a square on a maximum circle of the sphere.
- (\mathcal{C}_7) Rectangular: four $m = +1/2$ melting points sitting at the vertices of a rectangle on a maximum circle on the sphere. The bifurcate textures belonging to this class are defined by a scalar parameter ϱ_0 (see Table I). The two limiting configurations $\varrho_0 \rightarrow 0$ and $\varrho_0 \rightarrow \sqrt{(28\pi)/(5\bar{c})}$ correspond to \mathcal{C}_6 and \mathcal{C}_3 , respectively. Thus, as ϱ_0 tends to zero the melting points tend to locate at the vertices of a square on a maximum circle on the sphere, while as ϱ_0 increases the four $+1/2$ defects move on a maximum circle, approaching each other two by two until they collapse into two $+1$ defects.

As highlighted in Table I, these classes of bifurcate configurations are linear combinations of one, two or at most

three of the normal modes (7). All the bifurcate configurations but \mathcal{C}_7 are characterized solely by the moduli ϱ_h of the complex coefficients A_h , while the arguments ψ_h are arbitrary. For the rectangular configuration (that is the only bifurcate state resulting from the linear combination of three normal modes; specifically, f_0 , f_1 and f_{-1}), the moduli of the coefficients A_0 , A_1 and A_{-1} are as in Table I, while the arguments are subject to the restriction $2\psi_0 - \psi_1 - \psi_{-1} = (2l + 1)\pi$, with $l \in \mathbb{Z}$. Therefore, for rectangular configurations only two out of the three arguments are completely arbitrary.

For the linear axisymmetric configuration the nematic texture varies as the argument ψ_0 varies. Indeed, $\psi_0 = 0$ corresponds to a uniform alignment along the parallels (purely bend phase), while $\psi_0 = \pi/2$ corresponds instead to a uniform alignment along the meridians (purely splay phase). For the monovalent and linear non-axisymmetric configurations the arbitrariness of the arguments reflects the invariance of these states under rigid rotations around the polar axis. Finally, for the bifurcate configurations resulting from a linear superposition of two or three normal modes, it can be proven that the invariance under rigid rotations around the polar axis reflects on the arbitrariness of one of the two arbitrary arguments, the other determines instead the texture.

As the determination of the topological charge m of a melting point located at the point p is concerned, we follow similar arguments as in [28] and find out that $m = m_\varphi + \oint_{\mathcal{C}} [\arg(q)]' s / (4\pi)$, where \mathcal{C} is a regular closed simple circuit that is oriented anti-clockwise around the normal to the sphere at p and can be continuously contracted to p , s denotes the arc-length along \mathcal{C} , and the prime denotes differentiation with respect to s . The term m_φ is instead the topological charge of the reference field \mathbf{e}_φ , which vanishes wherever \mathbf{e}_φ has no singularity, that is at any point on the sphere except for the poles where it is equal to unity.

The dimensionless energies of the bifurcate configurations are reported in Table I. In agreement with the theoretical result in [29], the tetrahedral configuration \mathcal{C}_5 is the ground state. It is worth noting that the rectangular, squared and linear axisymmetric states have the same energy (see Figure 1). This implies that, at small temperature departures from T_{cr} , the rectangular configuration can vary continuously from the squared configuration to the linear axisymmetric one with no energy cost.

To determine the locally stable bifurcate solutions, we study the energy functional at temperatures slightly lower than T_{cr} . As observed above, at these temperatures the approximate equilibrium solutions are of the form (8) with $A_2 = 0$. This enables us to adopt the analytical approach introduced in [30]. Upon substitution of (8) and (7) into the energy functional, the stability analysis reduces to the determination of the local minima of a real-valued function \mathcal{W} in the four complex variables A_{-2} , A_{-1} , A_0 and A_1 . The stationary points of \mathcal{W} lead to the same equilibrium configurations that we have determined by means of the Lyapunov-Schmidt reduction.

Moduli of A_h				Melting points	Dimensionless energy
ϱ_{-2}	ϱ_{-1}	ϱ_0	ϱ_1	Topological charge and location	$W\bar{c}/(k\pi)$
$\frac{6}{5}\sqrt{\frac{2\pi}{\bar{c}}}$	-	-	-		$-\frac{36}{25}\varepsilon^4$
-	$\frac{3}{5}\sqrt{\frac{14\pi}{\bar{c}}}$	-	-		$-\frac{63}{25}\varepsilon^4$
-	-	$\sqrt{\frac{28\pi}{5\bar{c}}}$	-		$-\frac{14}{5}\varepsilon^4$
-	-	-	$\frac{3}{5}\sqrt{\frac{14\pi}{\bar{c}}}$		$-\frac{63}{25}\varepsilon^4$
$\frac{2}{5}\sqrt{\frac{14\pi}{3\bar{c}}}$	-	$\frac{4}{3}\sqrt{\frac{14\pi}{5\bar{c}}}$	-		$-\frac{644}{225}\varepsilon^4$
$\frac{2}{5}\sqrt{\frac{14\pi}{\bar{c}}}$	-	-	$\frac{4}{5}\sqrt{\frac{7\pi}{\bar{c}}}$		$-\frac{84}{25}\varepsilon^4$
-	$\sqrt{\frac{14\pi}{5\bar{c}}}$	-	$\sqrt{\frac{14\pi}{5\bar{c}}}$		$-\frac{14}{5}\varepsilon^4$
-	$\sqrt{\frac{28\pi - 5\varrho_0^2\bar{c}}{10\bar{c}}}$	$\in]0, \sqrt{\frac{28\pi}{5\bar{c}}}$	$\left[\sqrt{\frac{28\pi - 5\varrho_0^2\bar{c}}{10\bar{c}}}$		$-\frac{14}{5}\varepsilon^4$

Table I: The table is divided into three horizontal blocks (separated by double lines) relating, from top to bottom, to solutions resulting from the linear superposition of one, two and three normal modes. The first four columns report the values of the moduli ϱ_h of the complex coefficients in the linear combinations. The second last column displays locations of melting points on the spherical shell; the last column contains the dimensionless energies of the bifurcate configurations.

Therefore, the study of the positive definiteness of the Hessian matrices at the bifurcate configurations can tell us which bifurcate configuration is a local minimizer of \mathcal{W} . We have found that only the tetrahedral configuration is a local minimizer of \mathcal{W} . This means that only \mathcal{C}_5 is stable, the others are unstable (Figure 1).

The instability of the monovalent and linear non-axisymmetric configurations is not surprising as they have never been observed experimentally in non-chiral nematic shells, whereas they have been theoretically predicted and experimentally observed in chiral nematic shells [31, 32]. The linear axisymmetric configuration is unstable for non-axisymmetric perturbations which lead it towards the tetrahedral state. This is in agreement with the results in [2]. It must be said that the biva-

lent axisymmetric configuration can be stabilized by the non-uniformity of the shell thickness [33], or out-of-plane escapes of the director [2, 34]. Both aspects have not been considered in this paper. When the nematic director field is not constrained to be tangential, the configuration with two +1 disclinations is the ground state for sufficiently small particles [34].

In summary, we use the two-dimensional Landau-de Gennes theory to study the onset of the temperature-induced nematic ordering in spherical shells which are initially in the isotropic phase. This approach has the advantage of predicting the transition temperature as well as determining exactly the textures just below the critical temperature.

The critical temperature depends on the size of the

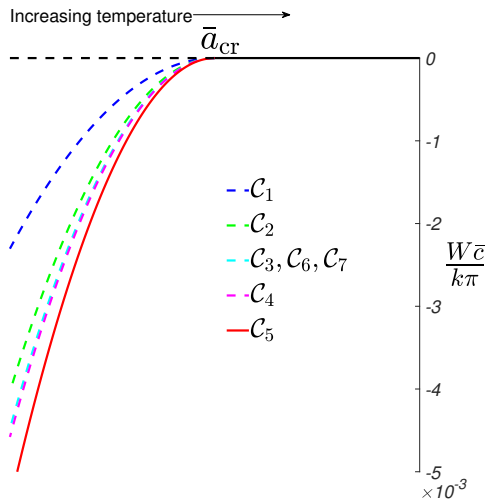


Figure 1: Energies of the bifurcate configurations. For small temperature departures from the critical value T_{cr} , the tetrahedral configuration (C_5) is a local minimizer of the energy functional. All the other configurations are unstable.

particle (c.f. equation (6)). Indeed, the extrinsic curvature lowers the isotropic-nematic transition temperature by a quantity proportional to the square of the ratio between the nematic coherence length $\sqrt{k/a_0}$ and the shell radius r . This effect is however negligible in the shells that are currently produced and used in the experiments. Typical radii of the nematic shells are of order of tens to hundreds of micrometers [14, 18], while the nematic co-

herence length is of order of nanometres. To appreciate the cooling effect of the extrinsic curvature, the shell radius should be at least one order of magnitude larger than the nematic coherence length. If this were the case, the extrinsic curvature of the shell would lower the isotropic-nematic transition temperature by 1%.

Far more interesting are the results on the nematic alignment at the critical temperature. The textures we have obtained by solving a generalized Thomson-like problem are expressed in closed form in terms of elementary trigonometric functions and reproduce different types of configurations. Some of these have been already predicted theoretically, found numerically, or observed experimentally. The total topological charge of the melting points obeys the Poincaré-Hopf theorem. The energy and stability analysis confirms that the tetrahedral configuration represents the ground state. Finally, the exact solutions we have here obtained can definitely be used as initial guesses in numerical investigations of more complex theories in which the fusion of the defect core and out-of-plane escape is considered simultaneously [34, 35].

Acknowledgements

This research has been partially supported by GNFM of Italian INDAM and by the PRIN 2017 research project (n. 2017KL4EF3) “Mathematics of active materials: from mechanobiology to smart devices”.

-
- [1] D. R. Nelson, *Nano Letters* **2**, 1125 (2002).
[2] V. Vitelli and D. R. Nelson, *Phys. Rev. E* **74**, 021711 (2006).
[3] P. Biscari and E. M. Terentjev, *Phys. Rev. E* **73**, 051706 (pages 6) (2006).
[4] M. A. Bates, *J. Chem. Phys.* **128**, 104707 (pages 4) (2008).
[5] H. Shin, M. J. Bowick, and X. Xing, *Phys. Rev. Lett.* **101**, 037802 (2008).
[6] M. A. Bates, G. Skacej, and C. Zannoni, *Soft Matter* **6**, 655 (2010).
[7] S. Kralj, R. Rosso, and E. G. Virga, *Soft Matter* **7**, 670 (2011).
[8] G. Napoli and L. Vergori, *Phys. Rev. E* **85**, 061701 (2012).
[9] G. Napoli and L. Vergori, *Phys. Rev. Lett.* **108**, 207803 (2012).
[10] A. Segatti, M. Snarski, and M. Veneroni, *Phys. Rev. E* **90**, 012501 (2014).
[11] D. Jesenek, S. Kralj, R. Rosso, and E. G. Virga, *Soft Matter* **11**, 2434 (2015), URL <http://dx.doi.org/10.1039/C4SM02540G>.
[12] L. Mesarec and W. G. A. I. S. Kralj, *Journal of Physics: Conference Series* **780**, 012015 (2017).
[13] A. Fernández-Nieves, V. Vitelli, A. S. Utada, D. R. Link, M. Márquez, D. R. Nelson, and D. A. Weitz, *Phys. Rev. Lett.* **99**, 157801 (2007), URL <https://link.aps.org/doi/10.1103/PhysRevLett.99.157801>.
[14] T. Lopez-Leon, V. Koning, K. B. S. Devaiah, V. Vitelli, and A. Fernandez-Nieves, *Nature Physics* **7**, 391 (2011), ISSN 1745-2473, URL <http://dx.doi.org/10.1038/nphys1920>.
[15] H.-L. Liang, E. Enz, G. Scalia, and J. Lagerwall, *Molecular Crystals and Liquid Crystals* **549**, 69 (2011).
[16] T. Lopez-Leon, A. Fernandez-Nieves, M. Nobili, and C. Blanc, *Phys. Rev. Lett.* **106**, 247802 (2011).
[17] G. Durey, Y. Ishii, and T. Lopez-Leon, *Langmuir* **36**, 9368 (2020).
[18] J. Noh, Y. Wang, H.-L. Liang, V. S. R. Jampani, A. Majumdar, and J. P. F. Lagerwall, *Phys. Rev. Research* **2**, 033160 (2020), URL <https://link.aps.org/doi/10.1103/PhysRevResearch.2.033160>.
[19] Y. Geng, J. Noh, I. Drevensek-Olenik, , R. Rupp, G. Lenzini, and J. P. F. Lagerwall, *Scientific Reports* **6**, 26840 (2016).
[20] J.-H. Kang, S.-H. Kim, A. Fernandez-Nieves, and E. Reichmanis, *Journal of the American Chemical Society* **139**, 5708 (2017), pMID: 28402658.
[21] A. Sharma, V. S. R. Jampani, and J. P. F. Lagerwall, *Langmuir* **35**, 11132 (2019), pMID: 31356088.
[22] V. S. R. Jampani, D. J. Mulder, K. R. De Sousa, A.-H. Gélébart, J. P. F. Lagerwall, and A. P. H. J. Schenning,

- Advanced Functional Materials **28**, 1801209 (2018).
- [23] A. Sharma and J. P. F. Lagerwall, *Liquid Crystals* **45**, 2319 (2018).
- [24] G. Napoli and L. Vergori, *International Journal of Non-Linear Mechanics* **49**, 66 (2013), ISSN 0020-7462, URL <http://www.sciencedirect.com/science/article/pii/S0020746212001461>.
- [25] M. Bowick and L. Giomi, *Advances in Physics* **58**, 449 (2009).
- [26] G. Napoli and L. Vergori, *J. Phys. A: Math. Theor.* **43**, 445207 (2010).
- [27] R. H. Rand and D. Armbruster, *Perturbation Methods, Bifurcation Theory and Computer Algebra* (Springer-Verlag, Berlin, Heidelberg, 1988), ISBN 0387965890.
- [28] R. Rosso, E. G. Virga, and S. Kralj, *Continuum Mechanics and Thermodynamics* **24**, 643 (2012), ISSN 1432-0959, URL <https://doi.org/10.1007/s00161-012-0259-4>.
- [29] T. C. Lubensky and J. Prost, *Journal de Physique II* **2**, 371 (1992).
- [30] G. Barbero and L. R. Evangelista, *An Elementary Course on the Continuum Theory for Nematic Liquid Crystals* (WORLD SCIENTIFIC, 2000), <https://www.worldscientific.com/doi/pdf/10.1142/3557>, URL <https://www.worldscientific.com/doi/abs/10.1142/3557>.
- [31] A. Darmon, O. Dauchot, T. Lopez-Leon, and M. Benzaquen, *Phys. Rev. E* **94**, 062701 (2016), URL <https://link.aps.org/doi/10.1103/PhysRevE.94.062701>.
- [32] A. Darmon, M. Benzaquen, S. Čopar, O. Dauchot, and T. Lopez-Leon, *Soft Matter* **12**, 9280 (2016).
- [33] V. Koning, T. Lopez-Leon, A. Fernandez-Nieves, and V. Vitelli, *Soft Matter* **9**, 4993 (2013).
- [34] G. Napoli, O. V. Pylypovskiy, D. D. Sheka, and V. Luigi, Submitted (2021).
- [35] A. L. Susser, S. Harkai, S. Kralj, and C. Rosenblatt, *Soft Matter* **16**, 4814 (2020).